A High-Throughput Continuous Spectroscopic Assay to Measure the Activity of Natural Product Methyltransferases

Hadas Simon-Baram[+],[a] Steffen Roth[+],[b] Christina Niedermayer,[b] Patricia Huber,[b] Melanie Speck,[b] Julia Diener,[b] Michael Richter,*[b] and Shimon Bershtein*[a]

Natural product methyltransferases (NPMTs) represent an emerging class of enzymes that can be of great use for the structural and functional diversification of bioactive compounds, such as the strategic modification of *C*-, *N*-, *O*- and *S*-moieties. To assess the activity and the substrate scope of the ever-expanding repertoire of NPMTs, a simple, fast, and robust assay is needed. Here, we report a continuous spectroscopic assay, in which *S*-adenosyl-L-methionine-dependent methylation is linked to NADH oxidation through the coupled activities of *S*-adenosyl-L-homocysteine (SAH) deaminase and glutamate dehydrogenase. The assay is highly suitable for a high-throughput evaluation of small molecule methylation and for determining the catalytic parameters of NPMTs under conditions that remove the potent inhibition by SAH. Through the modular design, the assay can be extended to match the needs of different aspects of methyltransferase cascade reactions and respective applications.

Introduction

Biocatalytic methylation by natural product methyltransferases (NPMTs) is one of the most prevalent biotransformations in nature. The methyltransferase (MT) activity of NPMTs almost invariably relies on *S*-adenosyl-L-methionine (SAM), a sulfonium compound that donates its activated methyl group to electron-rich *O*, *N*, *C*, or *S* accepting atoms.[1] Due to stereoelectronic effects,[2] methyl groups often lead to profound changes in biological and physical properties of small molecules, a phenomenon dubbed "the magic methyl effect".[3] Indeed, methylation was found to enhance binding selectivity and affinity of natural products, and to elevate their resistance to metabolic degradation.[4] Methylation was also shown to prolong half-life, improve solubility, and reduce toxicity of small molecules.[3,5] The importance of small molecule methylation in nature is manifested in the vast genomic and functional expansion of NPMT-encoding genes in organisms that carry-out highly specialized secondary metabolism, *e.g.*, production of flavonoids, alkaloids, and terpenoids in plants.[1,6] Given the importance of methylation in biosynthesis of natural products and secondary metabolites in nature, and the high potential of transmethylation reactions to improve the bioavailability, stability, and potency of small molecules, genomic and chemical profiling approaches have been developed to discover and engineer novel NPMTs and to expand the scope of methylated substrates.[7] These approaches, however, are hindered by two major limitations. First limitation, which concerns mostly preparative applications, is the necessity to recycle SAM due to its high cost and inherent instability. This limitation has been recently addressed by developing multi-enzyme *in vitro* systems that supply SAM by regenerating ATP and methionine productions,[8] or recycle SAM directly from the transmethylation reaction product, SAH.[9] Second limitation stems from the very narrow spectral change between SAM and SAH, which precludes a direct spectroscopic assessment of MT activity. The problem is further exacerbated by a potent product inhibition of most SAM-dependent MTs by the accumulating SAH.[10] Multiple *in vitro* coupled-enzyme reactions that quantify SAH by converting it to chromogenic or fluorescent molecules, or to molecules that can be detected by shifts in UV absorbance have been reported.[7e] While all these assays successfully remove the SAH-induced product inhibition, they suffer from other drawbacks that preclude their wide use, particularly when a simple and reliable assay that can be easily scaled up to a high-throughput screen is needed. Specifically, the usefulness of the assays that convert SAH into homocysteine, a free thiol group of which can be later detected by either Ellman's reagent[11] or thiol-activated fluorescent reporter molecules,[12] is reduced due to their discontinuous nature (*i.e.*, they require two experimental steps). Additionally, cysteine residues present in the enzymes that carry out the coupled reactions in these assays may generate high background readings. Other assays rely on cleavage of the amine group from the nucleobase adenine moiety of SAH, a change that can be detected continuously through a drop in UV absorbance at 263–

[a] *H. Simon-Baram,[+] Dr. S. Bershtein*
Department of Life Sciences
Ben-Gurion University of the Negev
Ben-Gurion blvd 1, 8410501 Beer-Sheva (Israel)
E-mail: shimonb@bgu.ac.il
[b] *Dr. S. Roth,[+] C. Niedermayer, P. Huber, M. Speck, J. Diener, Dr. M. Richter*
Fraunhofer Institute for Interfacial Engineering and Biotechnology (IGB), Branch BioCat
Schulgasse 11a, 94315 Straubing (Germany)
E-mail: michael.richter@igb.fraunhofer.de
[+] *These authors contributed equally to this work.*

Supporting information for this article is available on the WWW under https://doi.org/10.1002/cbic.202200162

265 nm.[13] A disadvantage of these assays is their relatively low sensitivity due to the absorbance of biomolecules at 260–280 nm. Although this drawback was later overcome by developing a fluorescently labeled SAM analogue, such a molecule remains unavailable to most labs.[14] Yet another reported continuous enzyme-coupled assay uses ammonium released by deamination of adenine moiety of SAH to convert 2-oxoglutarate to glutamate with concomitant oxidation of NADH to NAD^+.[15] In brief, the assay is based on the cleavage of SAH by 5′-methylthioadenosine/*S*-adenosylhomocysteine nucleosidase leading to the formation of adenine and its direct deamination by a deaminase releasing ammonium, the final substrate for the NADH coupled glutamate dehydrogenase. This approach has substantially increased the assay's sensitivity and its suitability for the detection of MT activity towards peptide and DNA substrates had been shown. However, its major drawback is the requirement to express and purify three enzymes (in addition to a MT) that couple SAH formation to NADH reduction, making the assay establishment and calibration a complicated endeavor. Further, assays based on multiple protein components are also less suitable for high-throughput substrate screens due to potential enzyme inactivation throughout prolong incubations, susceptibility to changes in buffer compositions, or non-specific interactions with substrates/products.

Here, we present a high-throughput continuous assay for the rapid and reliable detection of MT activity for small molecules. The assay avoids most drawbacks of the previously reported *in vitro* enzyme-coupled assays. The assay is based on a three-enzyme cascade consisting of a MT, a *S*-adenosylhomocysteine deaminase, and a NADH-dependent glutamate dehydrogenase (Scheme 1). The MT-catalyzed reaction is coupled to selective deamination of the demethylated cofactor SAH through SAH deaminase. The released ammonium ions are used by glutamate dehydrogenase to catalyze the hydrolysis of NADH to NAD^+, a step that can be easily monitored by following a drop in absorbance at 340 nm with a microplate spectrophotometer at small volumes. We demonstrate the utility of the assay for the high precision determination of catalytic parameters (k_{cat}, K_M) of two representative natural product *O*-MTs, catechol-*O*-MT from *Rattus norvegicus* (*Rn*COMT),[8b] and its bacterial homologue SafC *O*-MT from *Myxococcus xanthus* (*Mx*SafC).[8b,16] Further, we show the assay's usefulness for the activity screening of *O*-MT *Mx*SafC and anthranilate *N*-MT from *Ruta graveolens*, *Rg*ANMT,[17] against a range of known and *potential* substrates at a high-throughput manner. Our data demonstrate that the proposed assay is a robust tool to measure MT activity with almost no limitation to the identity of the methylated substrate. In principle, the assay can be further expanded by the addition of an enzyme module that supplies SAM molecules to the transmethylation reaction starting from L-methionine and ATP production.[8c]

Results and Discussion

Establishing the coupled assay

To generate a reliable, simple, and efficient continuous enzymatic assay with a minimal number of components for the measurement of MT activity, we coupled SAH, the byproduct of MT reaction, with NADH oxidation by combining the activities

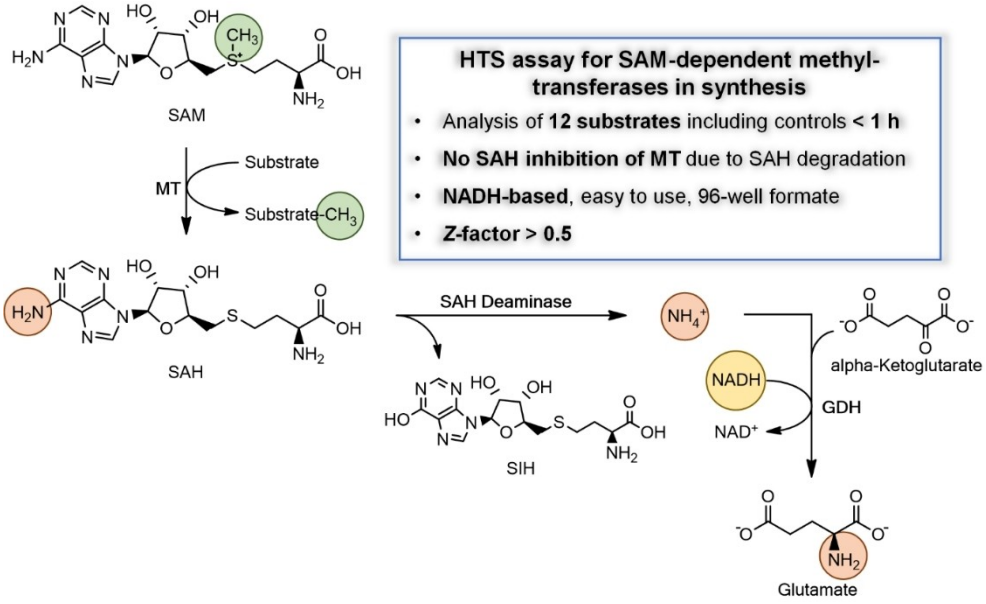

Scheme 1. Setup of a coupled assay to detect the enzymatic activity of methyltransferases based on the oxidation of NADH to NAD^+, which can be followed by the decrease in absorbance at 340 nm. During substrate methylation, the methyl group donor *S*-adenosyl-L-methionine (SAM) is converted to *S*-adenosyl-L-homocysteine (SAH). SAH serves as a SAH deaminase substrate to produce *S*-inosyl-L-homocysteine (SIH) and ammonia. Finally, glutamate dehydrogenase converts α-ketoglutarate and ammonium ions to glutamate while concomitantly oxidizing NADH (highlighted in yellow) to NAD^+. Methyl and amine groups transferred by catalysis are highlighted in green and orange, respectively.

of SAH deaminase from *Thermotoga maritima* (*Tm*MtaD)[18] and glutamate dehydrogenase from *Bos taurus*, (GDH) (see Scheme 1 and Experimental Section). We began by establishing the conditions that will ensure that MT activity is the rate limiting step of the coupled assay. This requirement is fulfilled when the steady-state velocity of SAH production by MT (v_{MT}) is slower than the steady-state velocity of ammonium production by SAH deaminase ($v_{SAH\ deaminase}$), and the latter, in turn, is slower still than the steady-state velocity of NADH oxidation by GDH (v_{GDH}), *i.e.*, $v_{MT} < v_{SAH\ deaminase} < v_{GDH}$. Under these conditions, and in the presence of excess amounts of SAM, α-ketoglutarate and NADH, SAH is converted almost instantaneously into SIH and ammonia; the latter, consequently, triggers an almost instantaneous oxidation of NADH. Thus, the rate of NADH consumption becomes a reflection of v_{MT}. To determine the validity of such a kinetic scheme, we, first, established that the rate of NADH oxidation by GDH is indeed linearly correlated with ammonium concentration at 0 to 150 μM range (Figure S1). Second, we determined whether SAH deaminase from *Thermotoga maritima* exhibits any promiscuous nucleosidase activity. Nucleosidase activity of *Tm*MtaD would lead to a degradation of SAH to adenine and *S*-(5-deoxy-D-ribos-5-yl)-L-homocysteine instead of formation of SIH and the release of ammonia. We found that *Tm*MtaD is highly selective and does not show any nucleosidase activity towards SAH under the assay's conditions (Figure S2A).

Under the assumptions of Michaelis-Menten kinetics, $v = k_{cat}[E][S]/(K_M + [S])$ [Eq. 1], where [E] and [S] are the concentrations of an enzyme and a substrate, respectively, the values of k_{cat} and K_M are constants that cannot be changed under given reaction conditions. However, maximal velocity (V_{max}), which is the product of k_{cat} and enzyme concentration [E], can be controlled by adjusting the enzyme concentration. Third, we determined the k_{cat} and K_M values of *Tm*MtaD and GDH for SAH and ammonia, respectively (Table 1 and Figure S3A), and inferred the enzymes' concentrations that under the steady-state rate of SAH deamination maintain the following inequality [Eq (1)]:

$$\frac{V_{max(TmMtaD)} \cdot [SAH]}{K_{M(TmMtaD)} + [SAH]} < \frac{V_{max(GDH)} \cdot [NH_4^+]}{K_{M(GDH)} + [NH_4^+]} \quad (1)$$

As demonstrated in Figure 1A, the molar ratio of 1:0.43 between *Tm*MtaD and GDH is expected to satisfy this condition for a wide range of SAH concentrations. Next, we validated experimentally that under the inferred conditions the rate of NADH oxidation is indeed coupled to SAH abundance. In consequence, we found a strong linear correlation between the reaction rate, as monitored by the decrease in absorbance at 340 nm, and SAH concentration at a 0–100 μM range (Figure 1B).

Having found the conditions for coupling *Tm*MtaD/GDH activities, we turned to determining the catalytic constants (k_{cat} and K_M) of catechol-*O*-MT from *Rattus norvegicus* (*Rn*COMT), and SafC *O*-MT from *Myxococcus xanthus* (*Mx*SafC) using L-dopamine as a substrate. To this end, the MT activity was coupled to *Tm*MtaD/GDH enzymatic cascade, and the steady-state (initial) velocities at a wide range of L-dopamine concentrations (0–700 μM) were obtained by following NADH oxidation at 340 nm. The derived catalytic constants for both MTs were in good agreement with those obtained from direct quantification of the products of the transmethylation reactions using HPLC-UV analysis, but only in the presence of SAH deaminase, which removes the SAH-induced inhibition (Figures S4–6 and Table 2). These findings clearly demonstrate that within the established enzymatic cascade, the steady-state velocity of transmethylation reactions is a rate-limiting step, which ultimately allows to accurately determine the catalytic parameters of MTs.

Table 1. Kinetic parameters of SAH deaminase for the conversion of SAH and of Glutamate dehydrogenase[19] for the conversion of NH_4Cl.

	K_M [mM]	k_{cat} [s-1]
SAH deaminase (TmMtaD)	0.18 ± 0.06	0.12 ± 0.01
Glutamate dehydrogenase	3.2	1 × 103

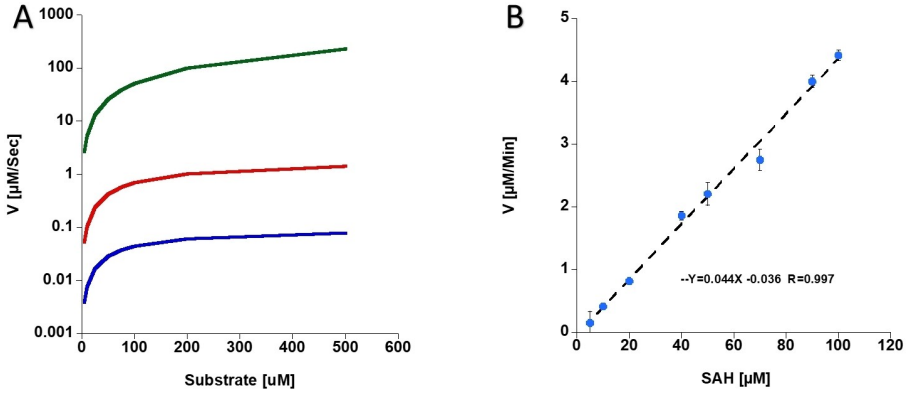

Figure 1. A. Calculated steady state velocities of GDH (green), SAH deaminase (red) and *Rn*COMT (blue). For any concentration of SAH catalyzed by SAH deaminase, an equivalent concentration of NH_4^+ is formed. As the rate of NH_4^+ consumption by GDH is higher than SAH consumption by SAH deaminase, GDH velocity is not limiting. Any MT can be added to this cascade, by adjusting the protein concentration so that $v_{MT} < v_{SAH\ deaminase}$. B. Linear range of SAH deaminase using SAH as substrate; y-axis: velocity μM/min; x-axis: concentration of SAH in μM. Error bars represent independent triplicates.

Table 2. Kinetic parameters of *Rn*COMT and *Mx*SafC for the methylation of dopamine.

	RnCOMT		MxSafC	
	K_M [μM]	k_{cat} [s-1]	K_M [μM]	k_{cat} [s-1]
Continuous assay	144 ±15	0.072 ±0.002	270 ±14	0.039 ±0.001
HPLC-UV without SAH deaminase	181 ±26	0.053 ±0.002	4000 ±1000	0.035 ±0.009
HPLC-UV with SAH deaminase	120 ±6	0.0490 ±0006	235 ±19	0.0340 ±0007

High-throughput MT activity screening

To demonstrate the applicability of the established coupled assay to conducting high-throughput substrate screening, we measured the activity of two representative small molecule MTs, SafC *O*-MT from *Myxococcus xanthus* (*Mx*SafC), and *N*-MT from *Ruta graveolens* (*Rg*ANMT), against a panel of twelve substrates comprised of phenolic acid derivatives (Table S1). *Mx*SafC participates in saframycin biosynthetic pathways wherein it efficiently and regioselectively methylates L-dopa, its physiological substrate, at 4′-*O* position.[16] In addition, *Mx*SafC was demonstrated to methylate other catechol derivatives, including catechol, dopamine, and caffeic acid.[8b] *Rg*ANMT takes part in biosynthesis of 1,3-dihydroxy-*N*-methylacridone by carrying out *N*-methylation of the methyl acceptor anthranilate.[17] *Rg*ANMT was found unreactive against an array of prospecting MT substrates, including aminobenzoic acid derivatives, phenol derivates, and purines, thus suggesting a very narrow specificity for anthranilate.[17]

The MT activity against a given substrate was determined by comparing the rate of drop in absorbance at 340 nm in the presence of all the components of the coupled assay with that obtained in the absence of MT. We note that we replaced SAH deaminase from *Thermotoga maritima* (*Tm*MtaD) with that from *Methanocaldococcus jannaschii* (*Mj*DadD), since, as we discovered, the catalytic efficiency (k_{cat}/K_M) of the latter is higher (Figure S3B, C). In similarity to *Tm*MtaD, *Mj*DadD does not exhibit any measurable nucleosidase activity (Figure S2B). The drop in signal in the absence of MT originates primarily from a spontaneous decomposition of NADH, which becomes apparent during prolonged measurements. However, unstable substrates that absorb at 340 nm might also contribute to a reduction in absorbance over time. As demonstrated in Figure 2A, the rate of NADH hydrolysis derived from the linear decay in signal in the presence of dopamine and *Mx*SafC was almost 5-fold faster than that achieved in the absence of *Mx*SafC, indicating that dopamine is a substrate of *Mx*SafC. Conversely, the rate of NADH hydrolysis in the presence of 2-aminophenethyl alcohol was not affected whatsoever by the removal of *Mx*SafC from the reaction mix, suggesting that 2-aminophenethyl alcohol is not a true substrate of *Mx*SafC (Figure 2B).

Using this approach, we screened the activity of *Mx*SafC against the panel of twelve compounds and found that, in addition to four known substrates, dopamine, caffeic acid, 3,4-dihydroxyhydrocinnamic acid and higenamine,[20] *Mx*SafC recognizes also novel substrates such as 6-hydroxydopamine hydrobromide and gallic acid (Figure 3, Figure S7, and Table S2). Methylation of the substrates identified by the coupled assay was further confirmed by HPLC-UV analysis (Figure S8).

Similarly, we measured the activity of *Rg*ANMT against the same set of twelve substrates and detected four substrates that were clearly recognized by the enzyme: 2-amino-5-bromophenol, 2-amino-5-nitrophenol, 2-amino-6-bromo-4-chlorophenol, and 2-amino-4-nitrophenol (Figure 4, Figure S9, and Table S3).

All the methylated substrates were further confirmed by HPLC-UV analysis (Figure S10). For dopamine and caffeic acid, direct evidence of methylation was provided using standards. 2-Aminophenethyl alcohol was detected in HPLC-UV as a substrate for *Rg*ANMT, but only after a prolong incubation time of 24 h, indicating that the MT activity was too low to be

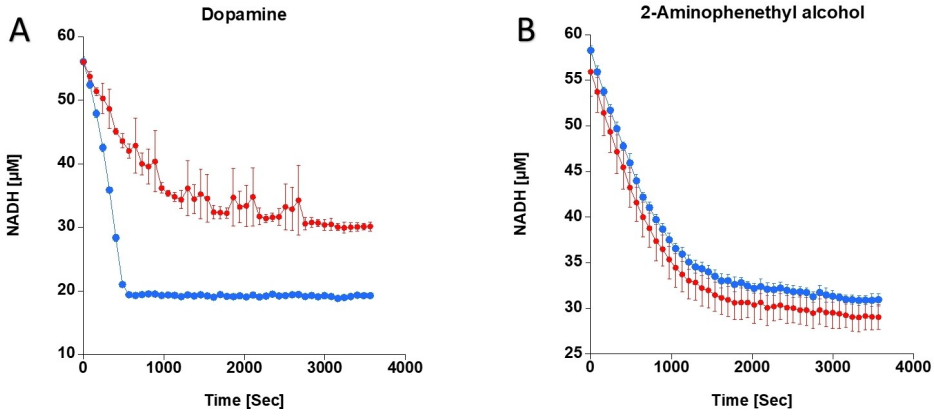

Figure 2. A. Conversion of dopamine and B. 2-aminophenethyl alcohol by *Mx*SafC. The reaction progress is followed by decreasing absorbance at 340 nm, which is converted to [NADH]; y-axis: NADH in μM; x-axis: Time in s; blue: complete sample setup; red: negative control w/o MT. N ≥ 3.

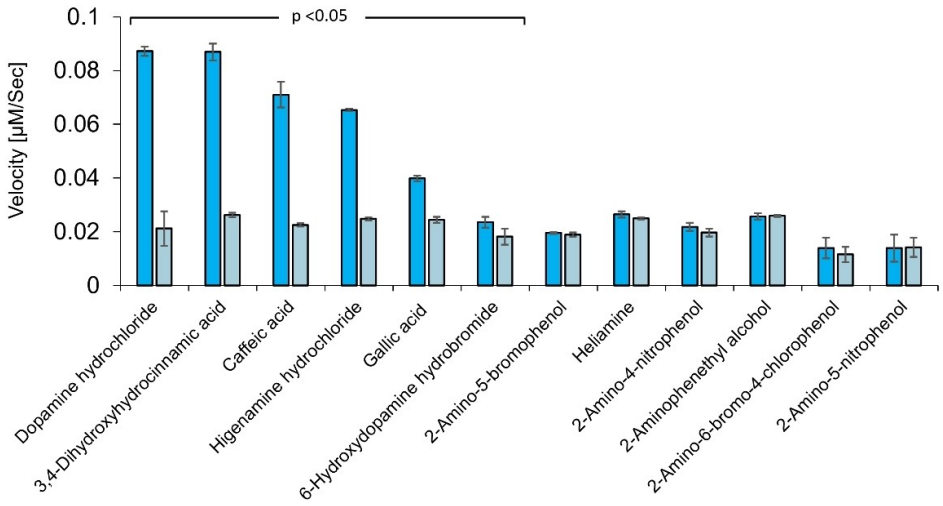

Figure 3. Changes of the initial velocity during the coupled assay indicate the substrate preference of *Mx*SafC. In blue samples velocity, in grey negative control of no *Mx*SafC, with substrates; y-axis: velocity µM/s; x-axis: substrates. Error bars represent SD of independent triplicates, p value < 0.05 using 1 tailed, paired students t-test.

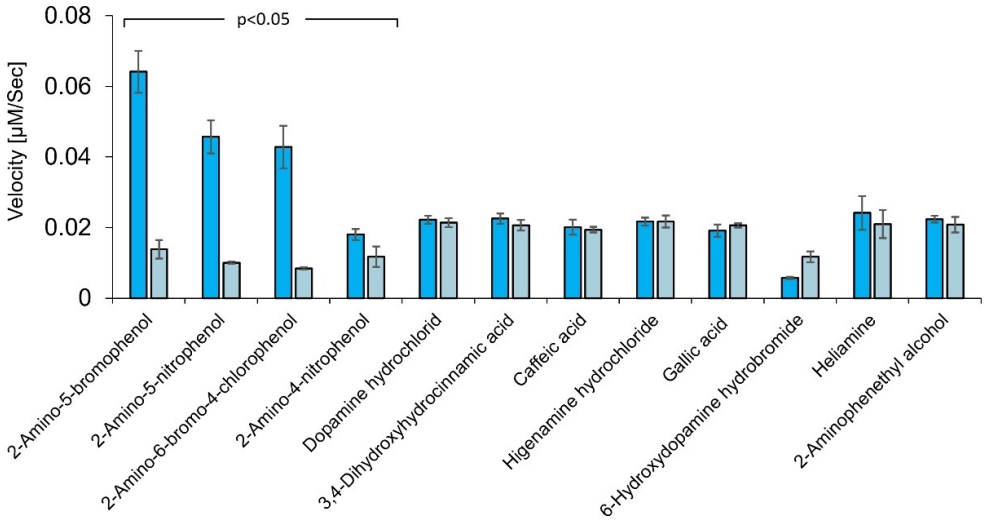

Figure 4. Changes of the initial velocity during the coupled assay indicate the substrate preference of *Rg*ANMT. In blue samples velocity, in grey negative control of no *Rg*ANMT, with substrates; y-axis: velocity µM/s; x-axis: substrates. Error bars represent SD of independent triplicates. p value < 0.05 using 1 tailed, paired students t-test.

detected within 1 h. Overall, this screen that was performed in a high-throughput manner using microtiter plate spectrophotometer, has successfully identified not only the known substrates of *Mx*SafC MT, but also previously unknown substrates of both *Mx*SafC and *Rg*ANMT. Importantly, we were able to detect MT activity towards substrates that absorb at 340 nm, such as caffeic acid, 2-amino-4-nitrophenol and 2-amino-5-nitrophenol (Figure 4), indicating that the spectroscopic properties of the substrates do not limit the usefulness of the assay to conduct high-throughput activity screens.

To determine the suitability of the developed assay for high-throughput screens (HTS), we calculated the *Z*-factor, which, while reporting on a dynamic signal range of an assay, also includes data variation associated with the signal measurements. Thus, the *Z*-factor indicates the quality and suitability of an assay for HTS screen.[21] The *Z*-factor for the developed HTS assay was calculated for *Mx*SafC as *O*-MT and for *Rg*ANMT as *N*-MT with L-dopamine and 2-amino-5-bromophenol, as reference substrates, respectively, using *Mj*DadD as deaminase (see Experimental Section). We found that the *Z*-factors for both assays were above 0.5, and therefore can be classified as "excellent assays"[21] (Table 3).

We were further interested if the deaminase (*Mj*DadD or *Tm*MtaD) would influence the *Z*-factor of the HTS assay. For that

Table 3. *Z*-factor analysis. Number of replicates n = 48, μ_p: initial velocity [μM/s] of sample with MT; μ_n: initial velocity [μM/s] of negative control w/o MT; SD, standard deviation.

MT	μ_p [μM/s]	SD μ_p	μ_n [μM/s]	SD μ_n	*Z*-factor
*Mx*SafC	0.062	0.001	0.029	0.001	0.82
*Rg*ANMT	0.053	0.003	0.019	0.001	0.68

reason, we performed the HTS assay with *Mx*SafC and dopamine as a substrate with both deaminases and calculated the *Z*-factor of each HTS assay. No significant difference between the *Z*-factors of the HTS assay using *Mj*DadD (Z-factor = 0.82) or *Tm*MtaD (Z-factor = 0.83) was observed (Table S4). For this reason, we conclude that both deaminases can be used for the detection of MT activity by the developed HTS assay.

Limitation of the assay

As discussed in the previous section, the utility of the coupled assay to detect novel MT activity is not diminished by the spectroscopic properties of the substrates. However, the ability of the assay to precisely measure the catalytic parameters of MTs can potentially be hindered in those instances where either the substrate and/or the product of a transmethylation reaction absorbs strongly at 340 nm. For example, ferulic and *trans*-isoferulic acids, which are the products of 3′-O and 4′-O methylation of caffeic acid, respectively, absorb less at 340 nm then caffeic acid (Figure 5). In this case, the change in absorbance at 340 nm, as measured by the coupled assay over time, becomes a convoluted signal originating not only from NADH oxidation, but also from a drop in caffeic acid concentration as well as from accumulation of the products of the transmethylation reaction. Thus, determination of catalytic parameters of small molecule MTs using our assay is limited to only those substrate/product pairs that do not absorb significantly at 340 nm.

Conclusions

Small molecule methylation catalyzed by SAM-dependent NPMTs carries a tremendous potential to improve bioactivity and bioavailability of natural products. The recognition of such a potential is manifested in the continuing effort to develop genetic tools to uncover and expand the arsenal of the available NPMTs and to engineer MTs with novel properties. To assist in this effort, here we presented a simple and reliable assay that allows high-throughput screen of MT activity virtually without limitation to the source of NPMTs, identity of the methyl accepting groups (O–, N–, C, or S–), or the spectroscopic properties of the potential substrates. Our assay overcomes several important limitations of the previously published assay. First, this is a one-step continuous assay that can be easily scaled to high-throughput measurements and its suitability for HTS has been proven by excellent *Z*-factors values > 0.5 for *O*-MTs and *N*-MTs. Second, in addition to a MT, the assay is based on only two additional enzymes. One of the enzymes, SAH deaminase, is highly expressed and easily purified, whereas the other, GDH, is commercially available. Third, the assay does not require fluorescently modified substrates and can be conducted in any lab equipped with a microtiter plate spectrophotometer. Lastly, we demonstrate that the assay is highly precise in determining the catalytic constants of methyl transfer for those substrates/products pairs that do not absorbs significantly at 340 nm.

Experimental Section

Reaction reagents: Glutamate dehydrogenase (GDH) (G2626-20MG), α-ketoglutaric acid (K1128), NADH (N8129) and SAM (A7007) were purchased from Sigma Aldrich. SAM was dissolved in 10 mM H_2SO_4, flash frozen in liquid nitrogen and stored in −80 °C for up to 2 months to prevent hydrolysis. NADH were dissolved in water at the same day of experiment, to prevent rapid hydrolysis. For Michaelis-Menten measurements, dopamine (H8502, Sigma) was dissolved in water to reach 100 mM, flash frozen in liquid nitrogen and stored in −80 °C. For High-throughput MT activity screening, stock solutions (100 mM) of the substrates (Table 4) were

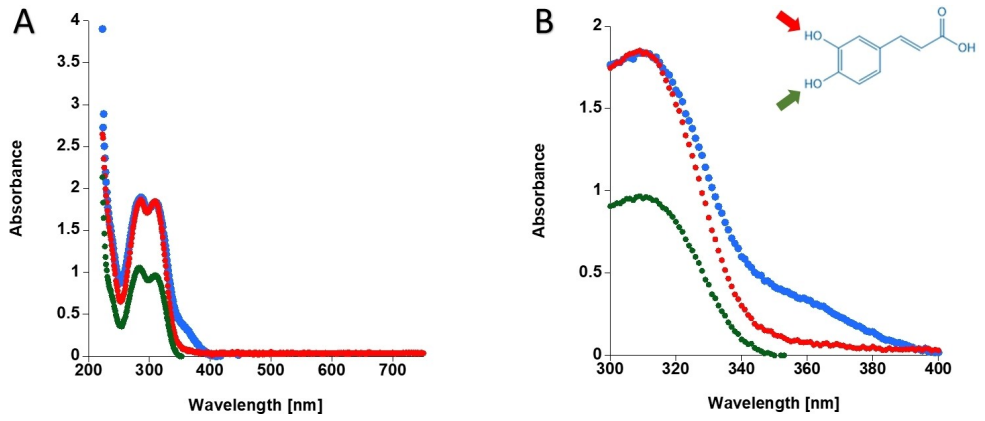

Figure 5. Left: UV-Vis spectra of caffeic acid (blue), ferulic acid (red) and trans-isoferulic acid (green) in the range of 200 to 750 nm. Right: Zoomed segment of caffeic acid, ferulic acid and trans-isoferulic acid in the range of 300 to 400 nm; y-axis: absorbance; x-axis: wavelength [nm].

Table 4. Overview of substrates and stock solutions for the MT activity screening.

Substrate	Supplier	Solvent for 100 mM stock solution
Gallic acid	Sigma (G7384)	EtOH
Caffeic acid	Sigma (C0625)	DMSO
3,4-Dihydroxyhydrocinnamic acid	Sigma (102601)	DMSO
6-Hydroxydopamine HBr	Sigma (162957)	H_2O
2-Aminophenethyl alcohol	Sigma (192600)	DMSO
2-Amino-5-bromophenol	Fluorochem (064750)	EtOH
2-Amino-4-nitrophenol	Sigma (A70402)	EtOH
2-Amino-6-bromo-4-chloro-phenol	Sigma (741485)	DMSO
2-Amino-5-nitrophenol	Alfa Aesar (B20870)	EtOH
Dopamine	Merck (8.22073)	H_2O
Heliamine	Sigma (291919)	H_2O
(±)Higenamine	Sigma (SML2313)	5 mM stock solution in H_2O

prepared in different solvents, pre-diluted to 5 mM in H_2O before their use in MT activity screening assays and stored at −20 °C.

Cloning and protein expression: *Rn*COMT was purified according to [8b]. The *E. coli* codon-optimized genes of *Tm*MtaD, *Mx*SafC and *Rg*ANMT were synthesized by BioCat Gen Synthesis - BioCat GmbH. *Mj*DadD was kindly provided from University Freiburg (Germany). For gene expression, pET22b plasmids carrying *Mx*SafC or *Rg*ANMT and pET28a plasmid carrying *Mj*DadD were transformed into *E. coli* BL21 (DE3), the pET22b plasmid carrying *Tm*MtaD was transformed into *E. coli* Rosetta (DE3) pLysS by electroporation. The cells were maintained on LB agar containing ampicillin (100 μg/mL, pET22b constructs) or kanamycin (30 μg/mL, pET28a constructs). Single colonies were used to inoculate LB precultures containing the corresponding antibiotic and cultivated at 37 °C, 20 h, 150 rpm agitation in shake flasks. For the main cultures LB media containing the corresponding antibiotic were inoculated to an initial optical density of 0.2 (OD_{600}) from preculture and incubated at 37 °C, 150 rpm agitation until an OD_{600} of 0.5 to 0.8 was reached. Protein production was induced by the addition of isopropyl β-D-1-thiogalactopyranoside (IPTG, 0.2 mM for MTs, 0.25 mM for *Mj*DadD and 0.1 mM for *Tm*MtaD plus 0.1 mM $ZnSO_4$) and cells were cultivated for additional 20 h at 20 °C, 150 rpm agitation for MTs and 4 to 5 h at 37 °C, 150 rpm agitation for deaminases, respectively. Afterwards, cells were harvested by centrifugation (5,000×g, 5 min, 4 °C) and stored at −20 °C. Cell pellets were resuspended (5 ml buffer per 1 g pellet) in lysis buffer (*Mx*SafC and *Rg*ANMT 40 mM TRIS HCl buffer pH 8.0, 100 mM NaCl, 20 mM imidazole; *Tm*MtaD and *Mj*DadD 100 mM HEPES pH 7.5, 100 mM KCl, 20 mM imidazole) containing 0.1 mg/mL lysozyme and 0.01 mg/mL DNAseI and incubated for 30 min on ice. Cells were lysed by high-pressure homogenization (1.8 kbar, 4 °C) and cell lysates were clarified by centrifugation (30,000×g, 4 °C, 30 min). Next, the supernatant was loaded onto a Ni-NTA column and the column was washed with 10 column volumes (CV) of lysis buffer. For protein elution, the amount of elution buffer (*Mx*SafC and *Rg*ANMT 40 mM TRIS HCl pH 8.0, 100 mM NaCl, 500 mM imidazole; *Tm*MtaD and *Mj*DadD 100 mM HEPES pH 7.5, 100 mM KCl, 500 mM imidazole) was stepwise increased (*Mx*SafC, *Rg*ANMT and *Mj*DadD 8 CV 5% elution buffer, 8 CV 60% elution buffer, 8 CV 100% elution buffer; *Tm*MtaD 8 CV 1% elution buffer, 8 CV 60% elution buffer, 8 CV 100% elution buffer). Buffer conditions were adjusted to the final assay conditions using gravity flow PD10 columns. If necessary, protein solutions were concentrated using a spin column (10 kDa MWCO, 4.000×g, 8 min, 4 °C).

Linearity of glutamate dehydrogenase (GDH): Linearity of GDH depending on ammonia concentrations was analyzed under HTS assay conditions at various ammonia concentrations between 0 and 150 μM ammonium chloride. The final assay consisted of 50 mM potassium phosphate at pH 7.5 or pH 8, 50 mM KCl, 20 mM $MgCl_2$, 100 μM NADH, 500 μM α-ketoglutaric acid, and 0.85 μM glutamate dehydrogenase.

Nucleosidase activity of *Tm*MtaD towards SAH: The assay consisted of 50 mM potassium phosphate at pH 7.5, 50 mM KCl, 20 mM $MgCl_2$, 500 μM SAH, and 3.5 μM SAH deaminase. Samples were prepared, incubated for 1 h at RT and analyzed by HPLC-UV.

MT activity screening: The final assay consisted of 50 mM potassium phosphate (pH 7.5 or pH 8.0), 50 mM KCl, 20 mM $MgCl_2$, 100 μM NADH, 500 μM α-ketoglutaric acid, 0.85 μM glutamate dehydrogenase, 500 μM SAM, 3.5 μM *Mj*DadD SAH deaminase, 2 μM MT and 500 μM substrate in a total volume of 200 μL. SAM, substrate, and MT were pipetted into a microtiter plate. For a master mix, potassium phosphate at pH 7.5, KCl, $MgCl_2$, NADH, α-ketoglutaric acid, glutamate dehydrogenase and SAH deaminase were combined, and the reaction was initiated by adding the master mix. The reaction progression was followed by the linear drop in 340 nm absorbance. Using the Excel software, a linear trendline were fitted to the linear drop segment in the readout. The rates of change in absorbance (mOD/min) were extracted from the linear equation $y = -ax + b$ fitting ($-\mathbf{a}$ in the linear equation, $R^2 > 0.9$). Finally, the absorbance rate was converted to NADH oxidation velocity using NADH extinction coefficient 6220 $M^{-1}cm^{-1}$. Experimental replicates were averaged and compared with their corresponding negative control for higher oxidation velocity rate using students t-test ($p < 0.05$).

SAH deaminase Michaelis-Menten measurements: The final assay consisted of 50 mM potassium phosphate at pH 7.5, 50 mM KCl, 20 mM $MgCl_2$, 100 μM NADH, 500 μM α-ketoglutaric acid, 0.85 μM glutamate dehydrogenase, 2 μM of *Tm*MtaD or *Mj*DadD and SAH in the range of 0 to 2 mM in a total volume of 200 μL.

To start the reaction, 120 μL of master mix (containing all compounds except of SAH) were added to 80 μL of SAH. The reaction progression was followed by NADH oxidation at 340 nm as described in the MT activity screening section.

***Rn*COMT and *Mx*SafC Michaelis-Menten measurements in continuous assay**: The initial velocity was calculated for a range of dopamine concentrations (0–8 mM), saturated SAM (200 μM) and 2 μM of *Rn*COMT or *Mx*SafC. The final assay consisted of 50 mM HEPES pH 7.5, 100 mM KCl, 20 mM $MgCl_2$, 200 μM NADH, 500 μM α-ketoglutaric acid, 1.75 μM glutamate dehydrogenase, saturated SAM (200 μM), 4 μM *Tm*MtaD SAH deaminase, 2 μM MT and variable substrate concentration of dopamine in a total volume of 200 μL. The assay was performed at 25°C. To start the reaction, 150 μL of master mix (containing all compounds except of dopamine) were added to 50 μL of dopamine at variable concentrations. The reaction progression was followed by NADH oxidation at 340 nm as described in the MT activity screening section.

***Rn*COMT and *Mx*SafC Michaelis-Menten measurements in HPLC-UV**: The initial velocity was calculated for a range of dopamine concentrations (0–8 mM), saturated SAM (200 μM) and 5 μM of *Rn*COMT or *Mx*SafC. The final assay consisted of 50 mM HEPES pH 7.5, 100 mM KCl, 20 mM $MgCl_2$, saturated SAM (200 μM), 5 μM MT and variable substrate concentration of dopamine in a total volume of 200 μL with or without *Tm*MtaD SAH deaminase. The assay was performed at 25 °C. To start the reaction, 150 μL of

master mix (containing all compounds except of dopamine) were added to 50 µL of dopamine at variable concentrations. Aliquots were removed from the reaction mixes at various time points (up to 13 min, every 1 min), and the reactions were stopped by mixing with 10% perchloric acid at a 1:1 ratio. The aliquots were then centrifuged, and the supernatant was separated by high-performance liquid chromatography (HPLC) using a MultiHigh SCX 5-µm, 250- by 4.6-mm column (CS-Chromatographie Service GmbH, Germany). The mobile phase consisted of 400 mM ammonium fumarate (adjusted to pH 4.0 using formic acid) at a flow rate of 1 ml/min while measuring absorbance at 254 nm. Data analysis was performed by integrating the peaks corresponding to SAH or SIH (retention time 6.2 and 5.0 respectively) and fitting them to the corresponding calibration curves (Figure S4). The kinetic constants were derived by fitting the resulting data point to a Michaelis-Menten equation ($Vmax \cdot [S]/K_M + [S]$) using Kaleidagraph software.

Determination of *Z*-factor: The *Z*-factor for the developed HTS assay was calculated for *Mx*SafC as O-MT with L-dopamine and for *Rg*ANMT as N-MT with 2-amino-5-bromophenol. The assay was performed in 50 mM potassium phosphate at pH 7.5 or pH 8, 50 mM KCl, 20 mM $MgCl_2$, 100 µM NADH, 500 µM α-ketoglutaric acid, 500 µM SAM, 0.85 µM glutamate dehydrogenase, 500 µM substrate, and 2 µM *of Mx*SafC or *Rg*ANMT. The number of replicates was n = 48 for samples with MT and negative controls w/o MT. The Z-factor was calculated according to the following equation [Eq. (2)]:[21]

$$Z = 1 - \frac{3\,(SD\,\mu_p + SD\,\mu_n)}{|\mu_p - \mu_n|} \quad (2)$$

μ_p: mean of sample (for this assay: initial velocity of sample with MT)

μ_n: mean of negative control (for this assay: initial velocity w/o MT)

SD: standard deviation ($SD = \sqrt{\frac{\sum (x_i - \bar{x})^2}{n}}$) where n: Number of replicates

The HTS assays were classified depending on the value of their *Z*-factor, as follows:[21] $Z = 1$, an ideal assay; $1 > Z > 0.5$, an excellent assay; $0.5 > Z > 0$ A, a double assay; $Z = 0$, a "yes/no" type assay; $Z <$ 0,screening essentially impossible.

HPLC analysis: Samples were prepared by filtration using a spin column (MWCO 10 kDa) at 14.000×g for 10 min at 4 °C. The injection volume was 5 µL and chromatographic separation was achieved using a C18 Luna Omega-polar 100x2.1 mm, 1.6 µm column at a 0.45 mL/min flow rate and 30 °C. The column was equilibrated with an isocratic mixture of 10 mM ammonium formate at pH 3.0 (A) (98.5%) and acetonitrile (B) (1.5%). A gradient mixture was used from 0 to 2 min, where the composition changed from 98.5% A and 1.5% B to 97% A and 3% B. From 2 to 4 min from 97% A and 3% B to 94% A and 6% B. From 4 to 6 min 94% A and 6% B to 83% A and 17% B. From 6 to 12 min from 83% A and 17% B to 30% A and 70% B. From 12 to 12.17 min from 30% A and 70% B to 98.5% A and 1.5% B. Finally, an isocratic mixture was used from 12.17 to 15 min with an isocratic mixture of A (98.5%) and B (1.5%). For data evaluation, SAM and substrate decrease as well as SAH/SIH and product formation were monitored by a PDA detector at a wavelength of 220 nm and 254 nm.

Acknowledgements

E.coli *BL21(DE3) cells carrying the pMHT1* Tm*MtaD expression vector are a kind gift from Prof. Amir Aharoni and Prof. Dan Levi, Ben-Gurion University of the Negev, Israel. The plasmid pET28 carrying the* Mj*DadD gene was a kind gift from Prof. Jennifer Andexer, University of Freiburg, Germany. The authors acknowledge the Federal Ministry of Education and Research (BMBF, Germany) (161B0626 A) for M. R. and the Israel Ministry of Health (ERA-NET 5317) for S. B. for funding in frame of the 17-ERACoBioTech as part of the project BioDiMet: Methyl Transferases for the Functional Diversification of Bioactives.*

Conflict of Interest

The authors declare no conflict of interest.

Data Availability Statement

The data that support the findings of this study are available in the supplementary material of this article.

Keywords: biocatalysis · high-throughput screening · natural products · small molecule methyltransferases

[1] D. K. Liscombe, G. V. Louie, J. P. Noel, *Nat. Prod. Rep.* **2012**, *29*, 1238–1250.
[2] K. C. Chu, in *The Basis of Medicinal Chemistry/Burger's Medicinal Chemistry*; Wiley, New York **1980**, 393–418.
[3] H. Schonherr, T. Cernak, *Angew. Chem. Int. Ed.* **2013**, *52*, 12256–12267; *Angew. Chem.* **2013**, *125*, 12480–12492.
[4] a) A. W. Alberts, J. Chen, G. Kuron, V. Hunt, J. Huff, C. Hoffman, J. Rothrock, M. Lopez, H. Joshua, E. Harris, A. Patchett, R. Monaghan, S. Currie, E. Stapley, G. Albers-Schonberg, O. Hensens, J. Hirshfield, K. Hoogsteen, J. Liesch, J. Springer, *Proc. Natl. Acad. Sci. USA* **1980**, *77*, 3957–3961; b) A. Bahl, P. Barton, K. Bowers, M. V. Caffrey, R. Denton, P. Gilmour, S. Hawley, T. Linannen, C. A. Luckhurst, T. Mochel, M. W. Perry, R. J. Riley, E. Roe, B. Springthorpe, L. Stein, P. Webborn, *Bioorg. Med. Chem. Lett.* **2012**, *22*, 6694–6699; c) R. W. Friesen, C. Brideau, C. C. Chan, S. Charleson, D. Deschenes, D. Dube, D. Ethier, R. Fortin, J. Y. Gauthier, Y. Girard, R. Gordon, G. M. Greig, D. Riendeau, C. Savoie, Z. Wang, E. Wong, D. Visco, L. J. Xu, R. N. Young, *Bioorg. Med. Chem. Lett.* **1998**, *8*, 2777–2782.
[5] C. J. Smith, A. Ali, M. L. Hammond, H. Li, Z. Lu, J. Napolitano, G. E. Taylor, C. F. Thompson, M. S. Anderson, Y. Chen, S. S. Eveland, Q. Guo, S. A. Hyland, D. P. Milot, C. P. Sparrow, S. D. Wright, A. M. Cumiskey, M. Latham, L. B. Peterson, R. Rosa, J. V. Pivnichny, X. Tong, S. S. Xu, P. J. Sinclair, *J. Med. Chem.* **2011**, *54*, 4880–4895.
[6] a) L. Katz, R. H. Baltz, *J. Ind. Microbiol. Biotechnol.* **2016**, *43*, 155–176; b) S. Wang, S. Alseekh, A. R. Fernie, J. Luo, *Mol. Plant Pathol.* **2019**, *12*, 899–919.
[7] a) M. Z. Ansari, J. Sharma, R. S. Gokhale, D. Mohanty, *BMC Bioinf.* **2008**, *9*, 454; b) D. D. Baker, M. Chu, U. Oza, V. Rajgarhia, *Nat. Prod. Rep.* **2007**, *24*, 1225–1244; c) A. Barakat, A. Choi, N. B. Yassin, J. S. Park, Z. Sun, J. E. Carlson, *Gene* **2011**, *479*, 37–46; d) C. Li, R. Zhang, J. Wang, L. M. Wilson, Y. Yan, *Trends Biotechnol.* **2020**, *38*, 729–744; e) C. Zhang, S. A. Sultan, R. T, X. Chen, *Biores. Bioproc.* **2021**, *8*, 72.
[8] a) S. Mordhorst, J. Siegrist, M. Muller, M. Richter, J. N. Andexer, *Angew. Chem. Int. Ed.* **2017**, *56*, 4037–4041; *Angew. Chem.* **2017**, *129*, 4095–4099; b) J. Siegrist, S. Aschwanden, S. Mordhorst, L. Thony-Meyer, M. Richter, J. N. Andexer, *ChemBioChem* **2015**, *16*, 2576–2579; c) D. Popadic, D. Mhaindarkar, M. H. N. Dang Thai, H. C. Hailes, S. Mordhorst, J. N. Andexer, *RSC Chem. Biol.* **2021**, *2*, 883–891.

[9] C. S. Liao, F. P. Seebeck, *Nat. Catal.* **2019**, *2*, 696–701.
[10] R. Carmel, D. W. Jacobsen, in *Homocysteine in health and disease*, Cambridge University Press, Cambridge, **2001**.
[11] C. L. Hendricks, J. R. Ross, E. Pichersky, J. P. Noel, Z. S. Zhou, *Anal. Biochem.* **2004**, *326*, 100–105.
[12] C. Wang, S. Leffler, D. H. Thompson, C. A. Hrycyna, *Biochem. Biophys. Res. Commun.* **2005**, *331*, 351–356.
[13] K. M. Dorgan, W. L. Wooderchak, D. P. Wynn, E. L. Karschner, J. F. Alfaro, Y. Cui, Z. S. Zhou, J. M. Hevel, *Anal. Biochem.* **2006**, *350*, 249–255.
[14] E. S. Burgos, R. O. Walters, D. M. Huffman, D. Shechter, *Chem. Sci.* **2017**, *8*, 6601–6612.
[15] S. Duchin, Z. Vershinin, D. Levy, A. Aharoni, *Epigen. Chrom.* **2015**, *8*, 56.
[16] J. T. Nelson, J. Lee, J. W. Sims, E. W. Schmidt, *Appl. Environ. Microbiol.* **2007**, *73*, 3575–3580.
[17] B. Rohde, J. Hans, S. Martens, A. Baumert, P. Hunziker, U. Matern, *Plant J.* **2008**, *53*, 541–553.
[18] D. S. Hitchcock, H. Fan, J. Kim, M. Vetting, B. Hillerich, R. D. Seidel, S. C. Almo, B. K. Shoichet, A. Sali, F. M. Raushel, *J. Am. Chem. Soc.* **2013**, *135*, 13927–13933.
[19] C. Frieden, *J. Biol. Chem.* **1959**, *234*, 2891–2896.
[20] F. Subrizi, Y. Wang, B. Thair, D. Mendez-Sanchez, R. Roddan, M. Cardenas-Fernandez, J. Siegrist, M. Richter, J. N. Andexer, J. M. Ward, H. C. Hailes, *Angew. Chem. Int. Ed.* **2021**, *60*, 18673–18679.
[21] J. H. Zhang, T. D. Chung, K. R. Oldenburg, *J. Biomol. Screening* **1999**, *4*, 67–73.

Manuscript received: March 22, 2022
Revised manuscript received: July 1, 2022
Accepted manuscript online: July 4, 2022
Version of record online: July 14, 2022